

The LIGO's Nonsolved problems

(several remarks about the advanced version:
 $h \lesssim h_{SQL}$)

PART I (the first lecture)

Ia the thermal noise

Ib the excess noise

PART II (the second lecture)

IIa the noise from the actuator

IIb the problem of a new readout system.

Ia The thermal noise

Trivial classical condition for the simplest model:



$$F_{sz} = \frac{1}{2} h L m \omega_{gzav}^2 \geq \sqrt{4 k_B T H(\omega) \frac{1}{\tau_{avcz}}}$$

The signal $\underbrace{\hspace{10em}}$ depends on the confidence limit \uparrow Boltzmann constant \uparrow $\tau_{avcz} \geq \frac{2\pi}{\omega_{gzav}}$

$$h_{SQL} = \frac{2 \Delta X_{SQL}}{L} \approx \frac{1}{\pi L} \sqrt{\frac{\hbar \tau_{avcz}}{m}}$$

$$h_{SQL} \approx \frac{1}{3 \times 4 \cdot 10^5} \times \sqrt{\frac{10^{-27} \cdot 10^{-2}}{10^4}} \approx 2,5 \cdot 10^{-23}$$

$$F_{gzav} \approx 10^{-8} \text{ dyn} = 10^{-13} \text{ NEWTON}$$

$$H \lesssim 4 \cdot 10^{-5} \frac{\text{g cm}}{\text{sec}}$$

$\tau_{PEND}^* \geq 9 \cdot 10^{+8} \text{ sec}$

$H(\omega) = ?$

The big "mess":

1) $H = \text{const}$ (Viscous friction \rightarrow
 \rightarrow used in the Nyquist model)

2) $Q^{-1} = A \frac{\omega \tau_{\text{relax}}}{1 + (\omega \tau_{\text{relax}})^2}$ (Debye model)
($Q\omega \approx \text{const}$)

3) $Q^{-1} = \sum A^{(i)} \frac{\omega \tau_{\text{relax}}^{(i)}}{1 + (\omega \tau_{\text{relax}}^{(i)})^2}$ ("multi Debye")

\Downarrow
 $Q \approx \text{const}$

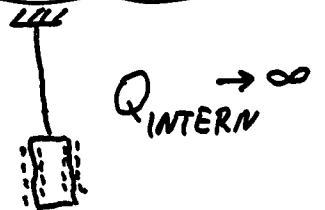
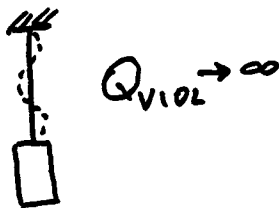
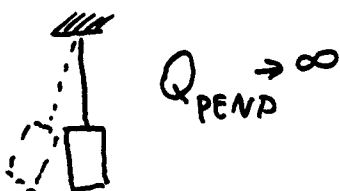
In real measurement:

$$H = H_{\text{viscouse}} + H_{\text{debye}} + H_{\text{surf}} + H_{\text{electz}} + H_{\text{magn}} + \dots$$

the cracks

the layers
at $H_2O, N_2 \dots$

the dust



sional mode being $\omega_{\text{sup}} \approx 4 \times 10^3$ rad/s) as a support and to use the torsional-pendulum mode of the cylinder oscillation which had $\omega_{\text{tors-pend}} \approx 2$ rad/s for the distance $2a \approx 2.5$ cm. Relatively simple calculations which we omit gave an estimate of the limit of $Q_{\text{tors-pend}}$ to the recoil losses at a level of 10^9 due for the above values of $\omega_{\text{tors-pend}}$ and ω_{sup} and with the mass of the cage $m_{\text{cage}} = 25$ kg.

All accumulated experience [3,4,6] of losses in fused silica fiber permits one to assume that a substantial part of the material losses may be described by the structural dissipation model [7]. According to this the Young's modulus Y and the shear modulus G of the material have imaginary parts which are independent of the frequency,

$$Y = Y_0(1 + i\phi_Y), \quad G = G_0(1 + i\phi_G),$$

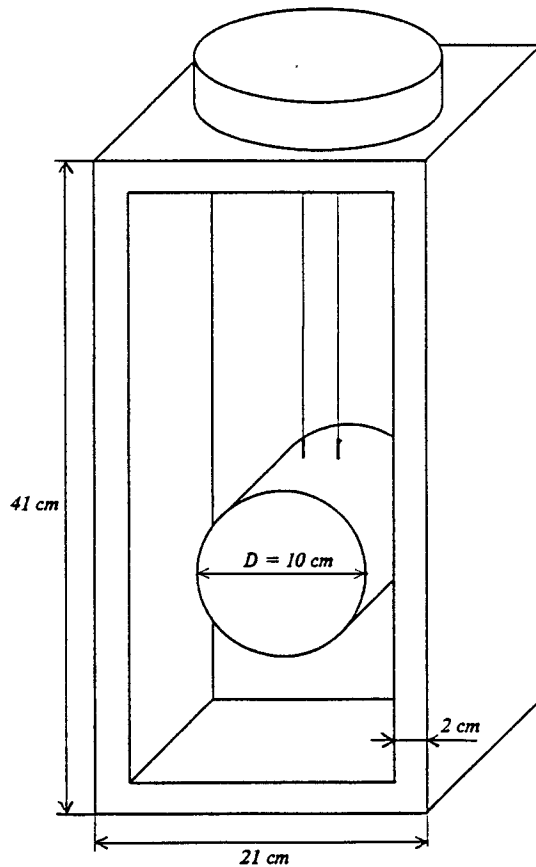


Fig. 1. Design of the pendulum and the suspension support structure.

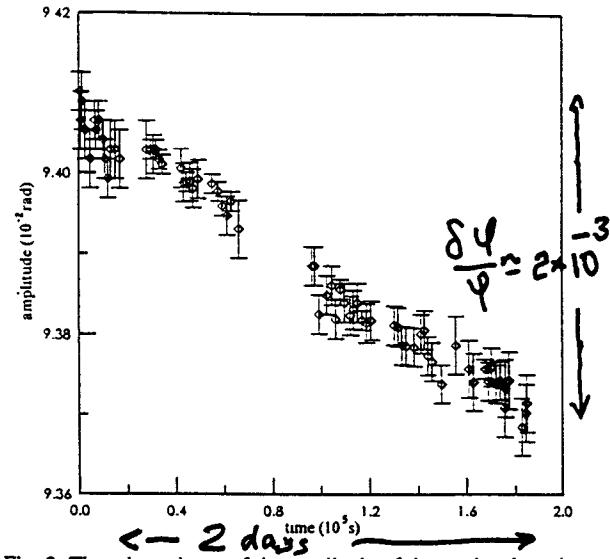


Fig. 2. Time dependence of the amplitude of the torsional-pendulum mode oscillation during a free decay.

where ϕ_Y and ϕ_G are the angles of losses in the material. These two values define $Q_{\text{tors-pend}}$,

$$Q_{\text{tors-pend}}^{-1} \approx \frac{\pi Gr^4}{Mga^2} \phi_G + \frac{1}{2l} \sqrt{\frac{\pi Yr^4}{2Mg}} \phi_Y,$$

where g is the gravitational acceleration, r the radius of the fibers. Substituting in this formula $\phi_Y = \phi_G = 1.4 \times 10^{-7}$ (see Ref. [5]), $a = 1.25$ cm, $r = 1 \times 10^{-2}$ cm, we can expect $Q_{\text{tors-pend}}^{-1} \approx 10^{-9}$ to be reached.

EXPECTED

In the described experiments four pendulum suspensions were tested, and the values obtained were $Q_{\text{tors-pend}} \approx (0.5-1) \times 10^8$. These values are more than one order smaller than the expected $Q \approx 10^9$. Additional losses could be explained as due to several small dust particles on the fiber's surface and due to the sedimentation of silica vapour on the surface of the fiber near the welding area.

Fig. 2 presents the measured time dependence of the amplitude of torsional-pendulum mode free oscillations in one of our tests. The recorded relative decrease of the amplitude 2×10^{-3} during two days corresponds to the relaxation time $\tau_m^* = 4.8 \times 10^7$ s ($\pm 10\%$). The gas pressure in the vacuum chamber was 2×10^{-6} Torr. Correcting for this pressure we obtain the excellent value $\tau_m^* \approx 1 \times 10^8$ s ≈ 3 years, which corresponds to $Q_{\text{tors-pend}} \approx 1 \times 10^8$ ($\pm 25\%$).

OBTAINED

Energy Dissipation in Violin Modes of the Test Mass Suspensions of Gravitational-Wave Antennas

Corresponding Member of the RAS V. B. Braginskii, V. P. Mitrofanov, and K. V. Tokmakov

Received May 17, 1995

One of the basic problems concerning the LIGO, VIRGO, and GEO-600 laser gravitational-wave antennas, which are currently being constructed (see, for example, [1]) is a suppression of the thermal motion of the centers of test masses (interferometer mirrors). The only method for solving this problem is to increase the quality factors Q of all the mechanical vibration modes that influence the motion of the test masses. According to the fluctuation-dissipation theorem, an increase in Q leads to a decrease in the spectral densities of the displacements of the centroid of a test mass away from the resonance frequencies of the mechanical vibration modes of the suspension and, consequently, to the possibility of detecting a broadband burst of gravitational radiation. The most important modes are those of the pendulum and violin vibrations in the suspension and the normal (internal) modes of a test mass (mirror) (see, for example, [2, 3]). This work reports the results of measurements of Q_{viol} for the violin vibration modes of the suspension of the test mass m that is close in value to the mass of the mirrors in the LIGO and VIRGO antennas. The development of a technique for the suspension of masses was aimed at the possibility of reaching and exceeding the so-called standard quantum limit (SQL) of sensitivity.

It is known that, at a sufficiently low level of dissipation (see, for example, [4]), the retroaction of the instrumental fluctuations (an inevitable consequence of the quantum theory) determines the sensitivity limit for the measurements of a force action on a test mass. If an instrument is continuously recording the coordinate of a mass during the time interval τ , and the acting force has the shape of a single period τ of a sinusoidal wave, then the SQL for the displacement amplitude of the test mass is

$$\Delta L_{\text{SQL}} = \frac{1}{2\pi} \sqrt{\frac{\hbar \tau}{m}}, \quad (1)$$

where \hbar is Planck's constant.

If the test mass is suspended by a thin filament of length l and total mass μ , then the rms displacement of the mass ΔL_{viol} , induced only by thermal vibrations in the violin modes of the filament, is

$$\Delta L_{\text{viol}} = \frac{1}{\pi^2 n^2} \frac{\mu}{m} \sqrt{\frac{2\pi k T l}{g Q_{\text{viol}}}}, \quad (2)$$

where k is the Boltzmann constant, T is the thermostat temperature, g is the free-fall acceleration, and n is the number of the violin mode ($n = 1, 2, 3, \dots$).

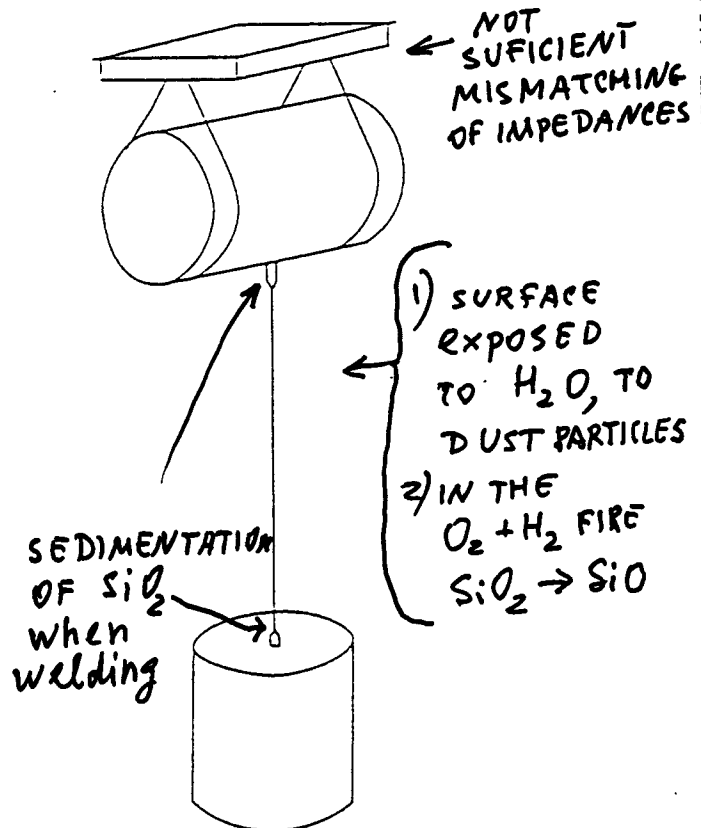


Fig. 1. Schematic of the test-mass suspension.

Thus, to achieve a high sensitivity of the antenna and, for instance, to satisfy the condition $\Delta L_{SQL} > \Delta L_{viol}$, we need the smallest possible value of μ and large values of Q_{viol} . In the measurements described below, we mainly applied the same technique as was used in the preliminary experiments [5]: the test mass and the suspension filament, including the upper part of its attachment, were made from fused silica. The filament was made from high-purity fused silica and, as a result, had low characteristic losses. It was welded to the test mass and to the upper part of the filament attachment.

In contrast with the preliminary experiments [5], where the values of Q_{viol} were measured in filaments with a small suspended mass ($m = 30$ g), in our experiments, we suspended a mass $m = 1.6$ kg, which is close to the mass of the mirror planned for the final version of the LIGO program. This significant increase in the mass made it necessary to use an intermediate element with a mass of approximately 2 kg in the suspension (Fig. 1.). This allowed us to suppress the leakage of the energy of the violin vibrations to the support.

The calculations of the insertion loss Q_{viol}^{-1} introduced by this leakage (they are not presented here) give an estimate of $Q_{viol}^{-1} \leq 10^{-11}$.

The second significant difference in our experiments from the preliminary ones is that the fused-silica filaments used were more heavily stressed. This made it possible for filaments with the diameter $D = 150 \mu\text{m}$ and length $l = 0.2$ m to have a rather small value of $\mu = 8 \times 10^{-3}$ g. The suspended mass induced the stress

$$\sigma = 4mg/\pi D^2 = 10^9 \text{ N/m}^2,$$

in these fibers, i.e., approximately 2% of the Young's modulus.

The Q -factor for the violin vibration modes Q_{viol} of strained filaments depends on their tension, which is determined by the suspended mass M and intrinsic losses in the filament material characterized by the loss angle φ_q :

$$Q_{viol}^{-1} = \frac{2}{l} \sqrt{\frac{YI}{Mg}} \left\{ 1 + \frac{(\pi n)^2}{2l} \sqrt{\frac{YI}{Mg}} \right\} \varphi_q, \quad (3)$$

where $I = \pi D^4/64$ is the moment of inertia for the cross section of the fused-silica filament, Y is the Young's modulus, and g is the free-fall acceleration.

The losses in the material were determined from the measured value of Q_{bend} , the Q -factor for the bending vibration modes of unloaded filament segments approximately 10 mm long with one end welded to a massive support. They were made from KS-4V analytical-purity fused silica with the lowest impurity concentration. In this case, $Q_{bend}^{-1} = \varphi_q$. Figure 2 shows the experimental values of Q -factors for lower modes of bending vibrations of the filaments. The curve is calculated for the case when the energy losses are determined only by the thermoelastic mechanism [6].

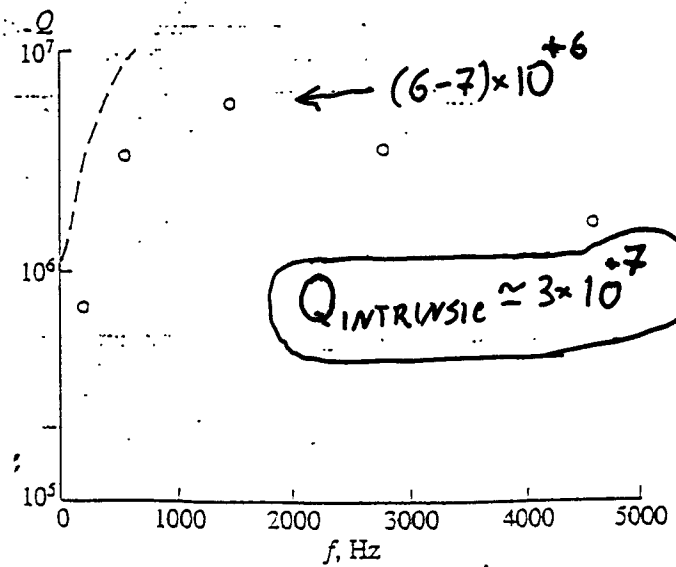


Fig. 2. Q -factors for lower modes of the bending vibrations of a fused-silica filament.

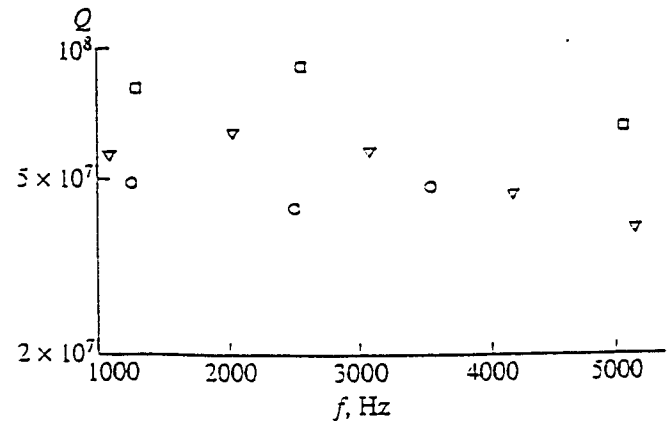


Fig. 3. Q -factors for violin vibration modes of the suspension filaments for three fused-silica pendulums.

The maximum of thermoelastic losses for the filaments under study was located near the characteristic frequency $f = 40$ Hz, so that, at frequencies above 1 kHz, thermoelastic losses made an insignificant contribution to the damping of bending vibrations of the filaments.

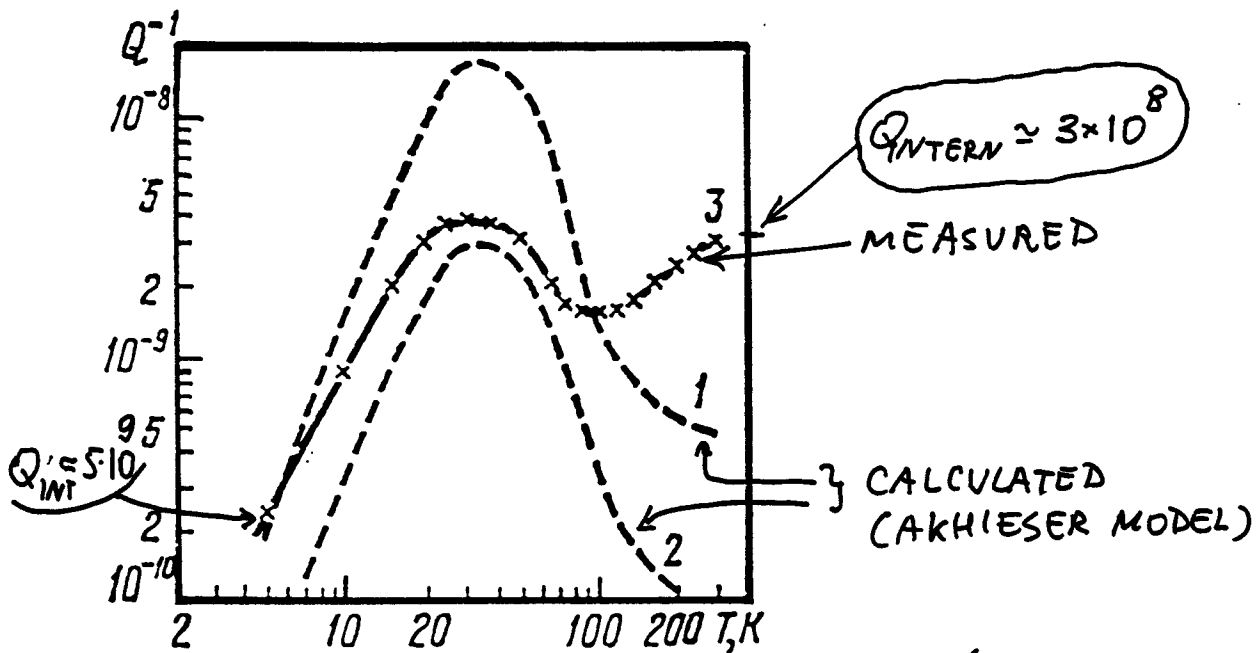
Substituting numerical values of the parameters into (3), we obtain the expected value of the Q -factor for violin vibration modes of the suspension filaments. $Q_{viol} = 2 \times 10^9$.

Figure 3 presents the values of the Q -factors for lower harmonics of the violin vibration modes of the suspension filaments, measured for the several pendulums that were studied. The statistical errors of the measurements were about 5%. The damping introduced by the energy transfer to the molecules of the residual gas in the vacuum chamber was

$$(Q_{viol}^{-1})_{res} = (5 \pm 2) \times 10^{-10}$$

FROM THE BOOK "SYSTEMS WITH SMALL DISSIPATION" Kip S. THORNE ED.

Resonators Made from Sapphire Monocrystals



Al₂O₃ CYLINDER, 38 kHz (V. MITROFANOV, L. OVODOVA,) 1980
m = 1 kg

measured (curves 1 and 2) and experimental (curve 3) temperature dependence of Q^{-1} for a sapphire resonator with vibration frequency of

pressure of less than 10^{-5} Torr.

quality factor was determined by measuring the damping

Conclusion of Ia part:

$$\left. \begin{aligned} 1) \quad (Q_{\text{pend}})_{\text{SiO}_2} &\approx 1 \times 10^8 \\ (Q_{\text{VIB}})_{\text{SiO}_2} &\approx 1 \times 10^8 \\ (Q_{\text{INTERN}})_{\text{SiO}_2} &\approx 3 \times 10^7 \\ (Q_{\text{INTERN}})_{\text{Al}_2\text{O}_3} &\approx 3 \times 10^8 \end{aligned} \right\}$$

these values
are neither ultimate
ones nor final ones.

2) $H(\omega)$ may not be accurately derived
from the values of Q ;

Only the floor of the noise from the
antenna may provide correct(?) values of $H(\omega)$?

The high Q give only a hope but
not a guarantee.

I b The excess noise

The thermal equilibrium is a grand illusion: the always existing free energy wants to "leak" → to redistribute itself in other forms. This process is always accompanied with the decrease of the total amount of free energy and with the rise of entropy.

Thus FD theorem is a correct one in the ultimate approximation only.

The simplest examples:

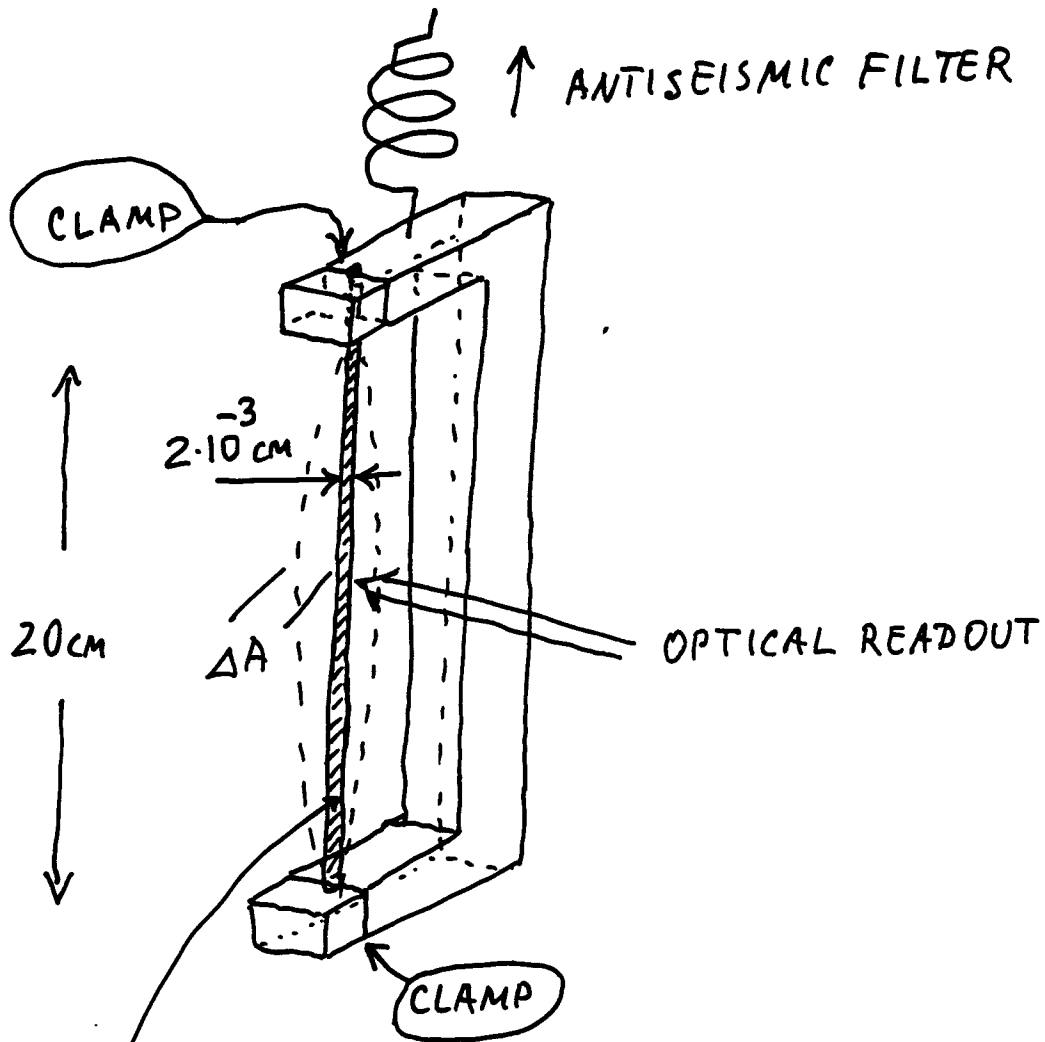
- 1) the acoustic emission from stressed solids
- 2) the random change of the size (of the dimensions) of solid bodies

For LIGO probably the most important are

- ① The excess noise in the violin modes of the suspension fibers.
- ② The random change of the mirrors diameter and length.
- ③ The croom noise from the last element of the antiseismic filter.

①

The sketch of the setup for the measurements of the Brownian motion of the suspension fiber (MSU group)



TUNGSTEN WIRE

$$\Delta A_{\text{BROWNIAN}} \approx 1,5 \times 10^{-9} \text{ cm}$$

$$\Delta A_{\text{READOUT}} \approx 2 \times 10^{-10} \frac{\text{cm}}{\sqrt{\text{Hz}}}$$

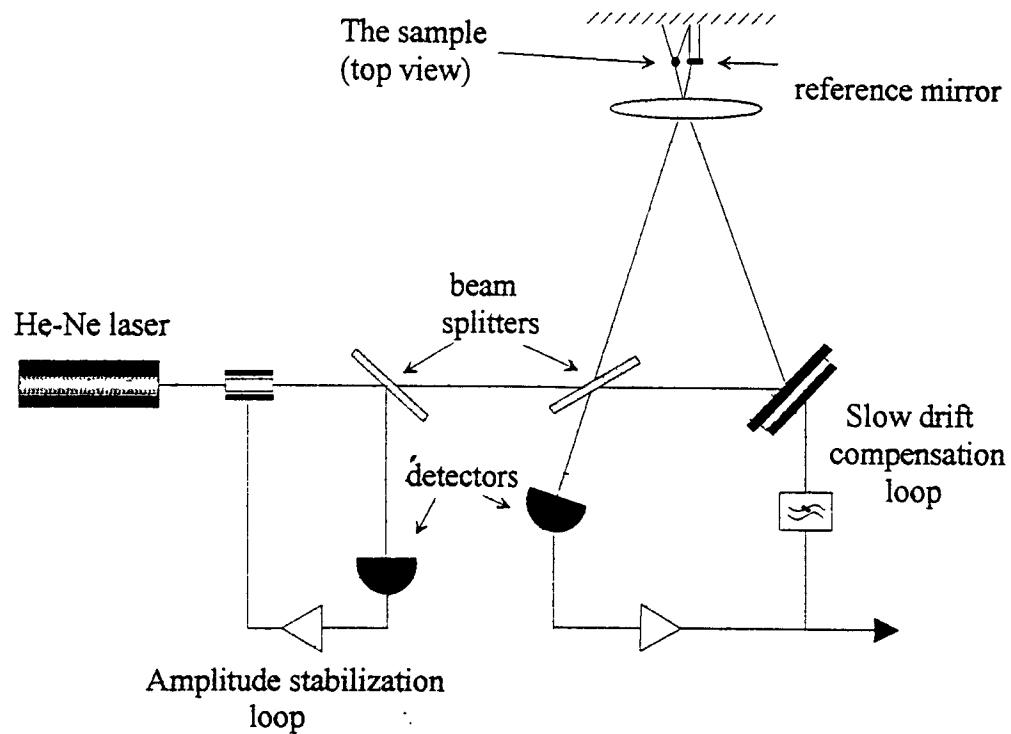


Figure 1.
The sketch of the measurement system.
(optical readout)

Sample number	Theory prediction (averaging time 30 s)	Well stressed samples			Intermediate stressed samples		Low stressed samples		
		1	2	3	4	5	6	7	8
Stress value, S/S_b		0.84	0.85	0.83	0.48	0.63	0.18	0.25	0.27
total data length, hrs		2	1.5	4	2.5	4	4.5	2	1
Number of the amplitude bursts overcoming the levels									
>3 \bar{A}	115 ± 15	343	306	217	236	155	112	126	72
>4 \bar{A}	25 ± 2	59	116	77	82	32	44	48	22
>5 \bar{A}	4 ± 4	12	36	16	20	4	15	16	4
>6 \bar{A}	0	9	13	3	4	0	2	4	0
>7 \bar{A}	0	6	2.5	0	0	0	0	1	0
>8 \bar{A}	0	6	0	0	0	0	0	0	0
>9 \bar{A}	0	6	0	0	0	0	0	0	0
>10 \bar{A}	0	6	0	0	0	0	0	0	0

Table 1. The results of the violin mode noise measurements on the tungsten wires. The S_b is a break point stress value for the samples, \bar{A} is the mean amplitude of oscillation.

Two types of noise:

1. Relatively long (≈ 1 min) and rare rise of the noise floor (above Brownian level)
2. Big bursts (peaks) which rate depends on the value of the stress.

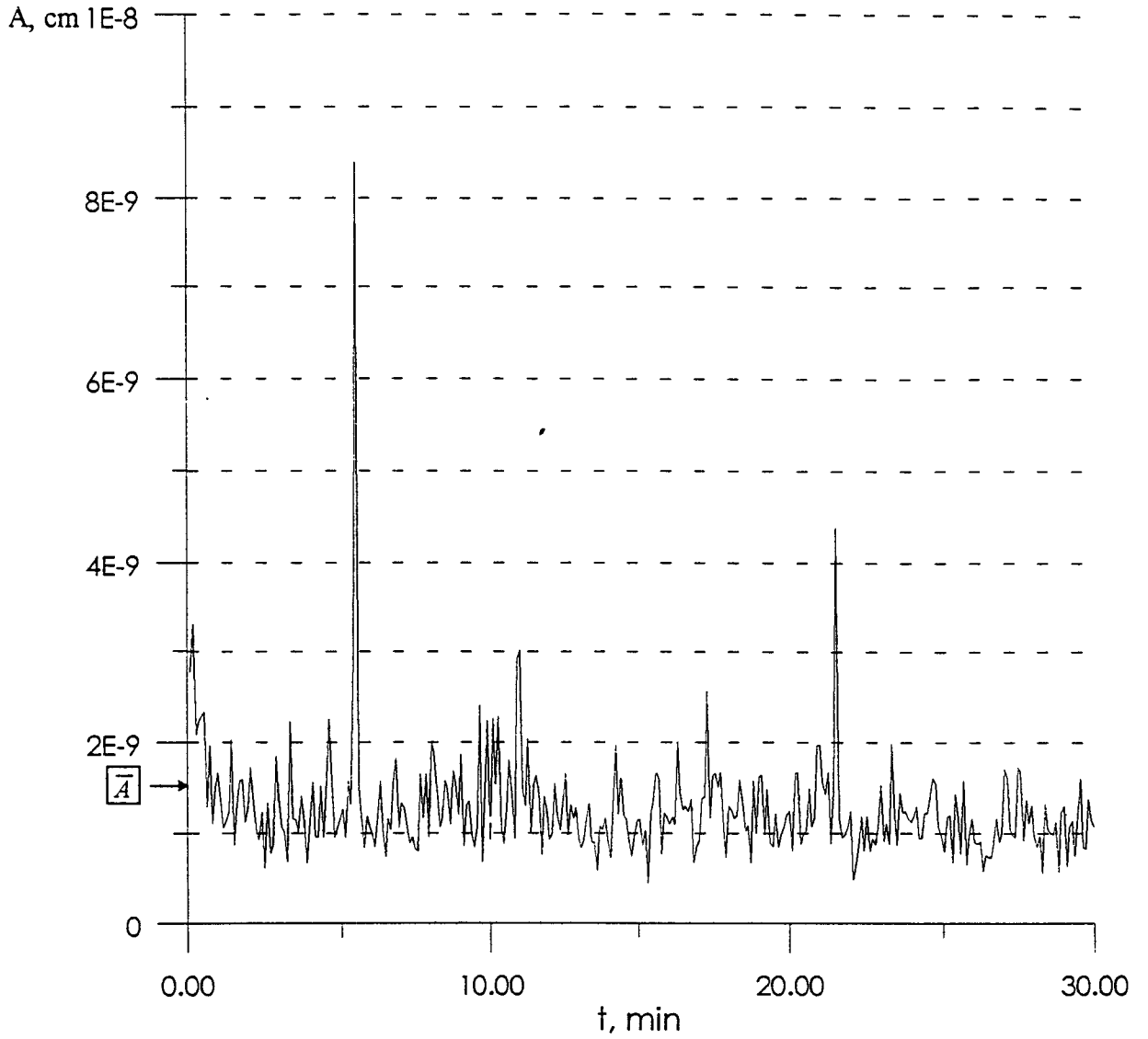


Figure 2.
 The time dependence of the oscillation amplitude for the well stressed sample of tungsten wire. Strain is 0.85 of break point value. The averaging time is 30 second.

\bar{A} is a theoretical prediction for the thermal noise mean amplitude.

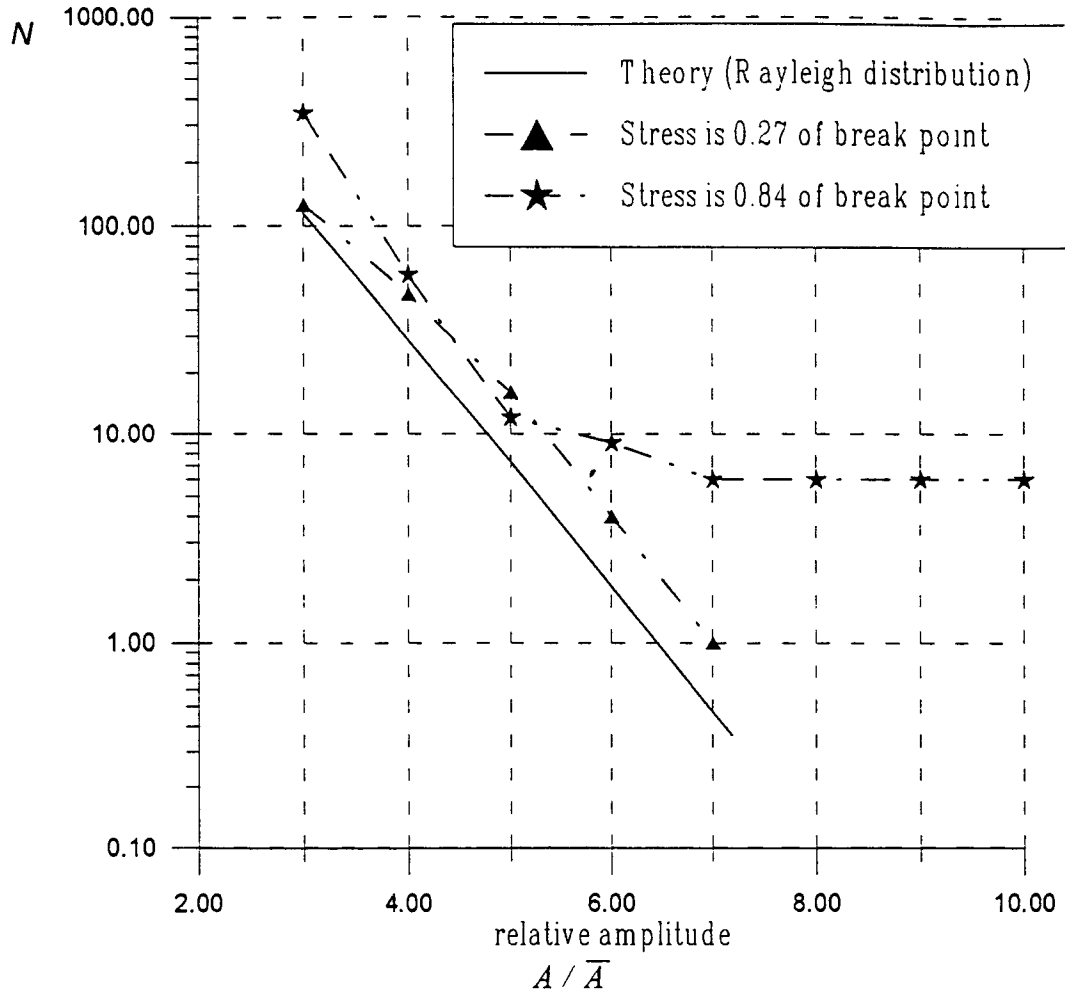


Figure 3.
The peak intensity histogram. N is the number of peaks per hour with the amplitude larger than A .

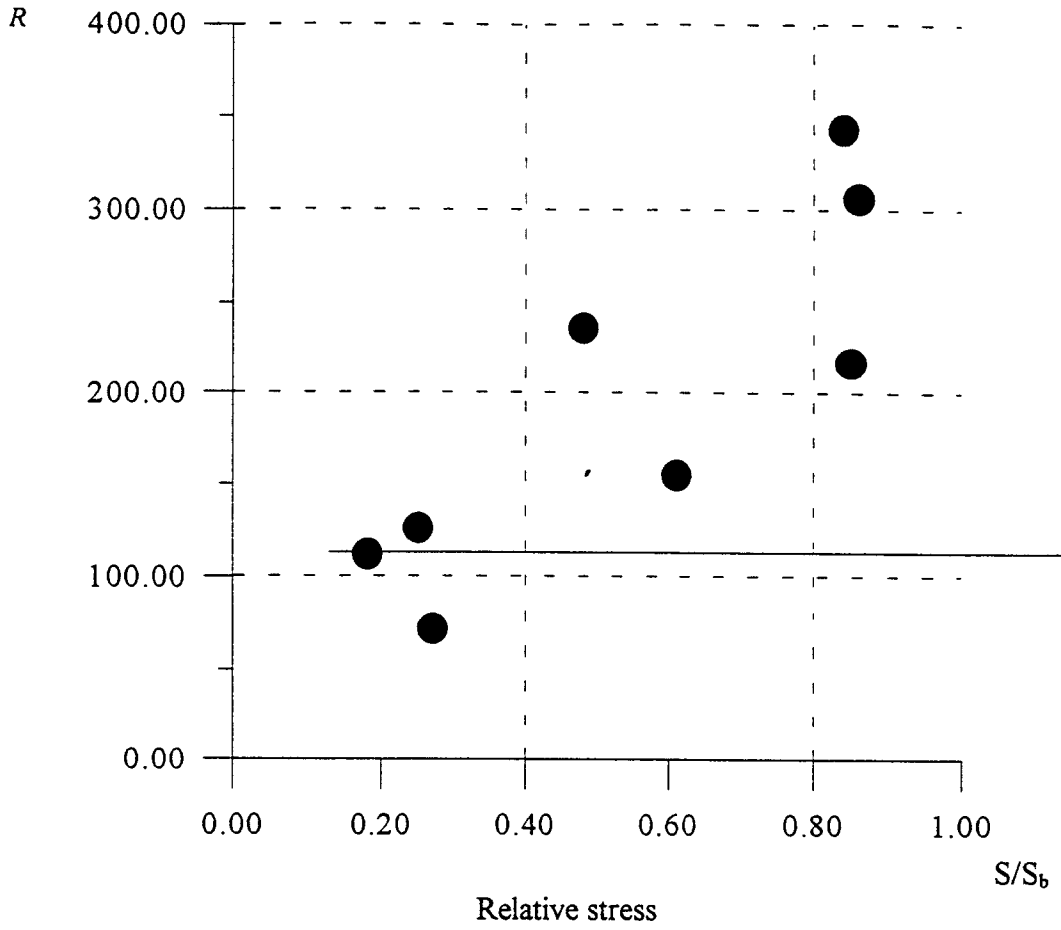


Figure 4.
 The dependence of excess peak rate R on the stress value. The peaks with the amplitude 3 times higher than the *rms* value are counted.
 Solid line is theoretical prediction for the thermal noise.

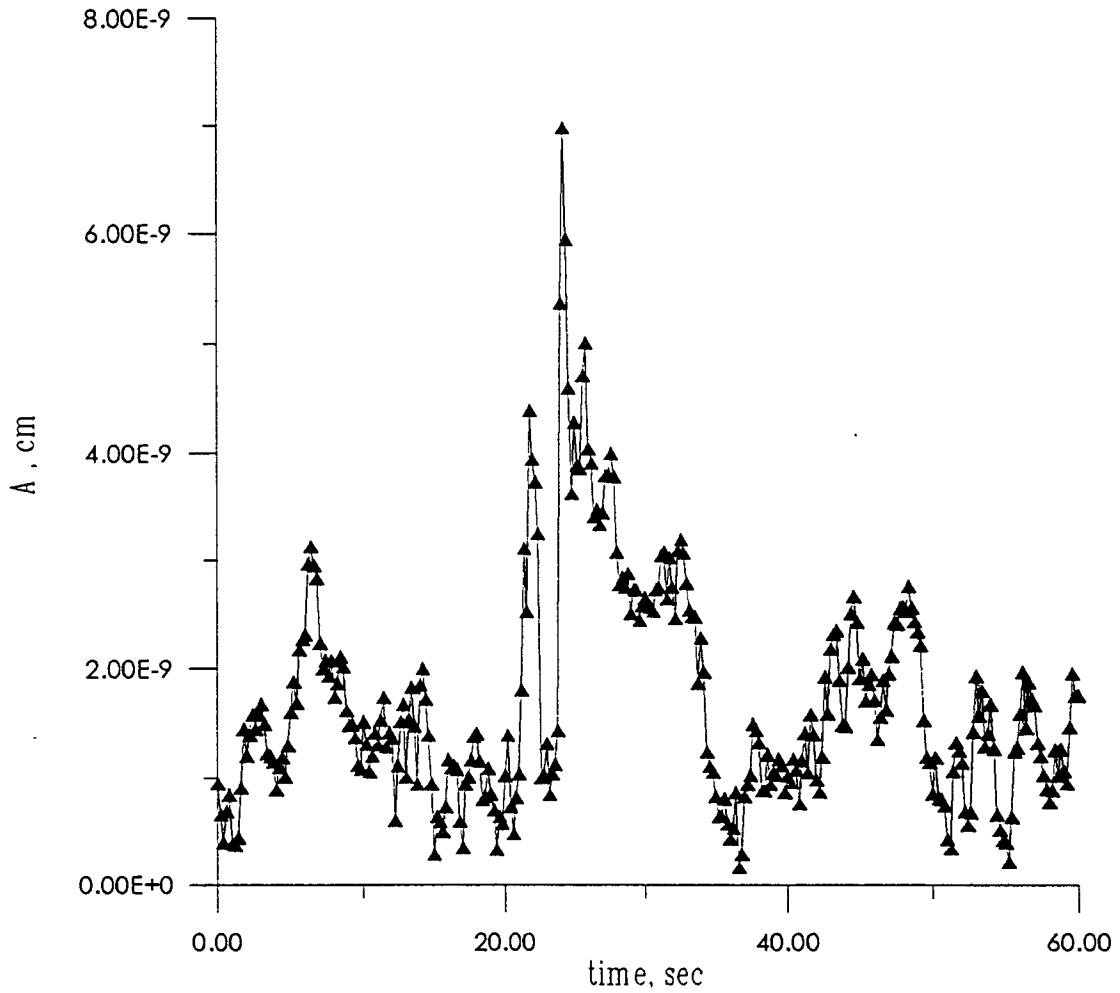
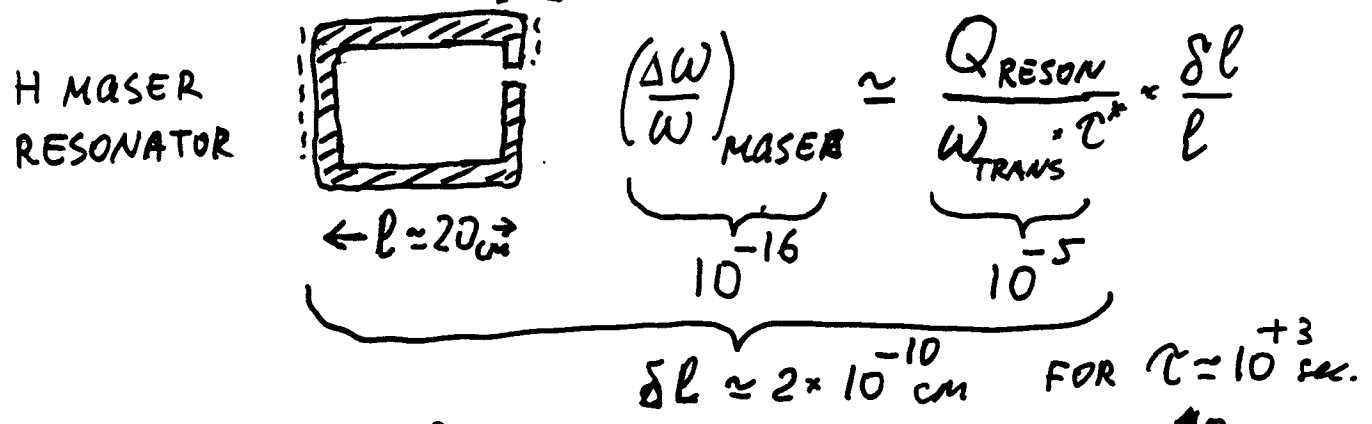
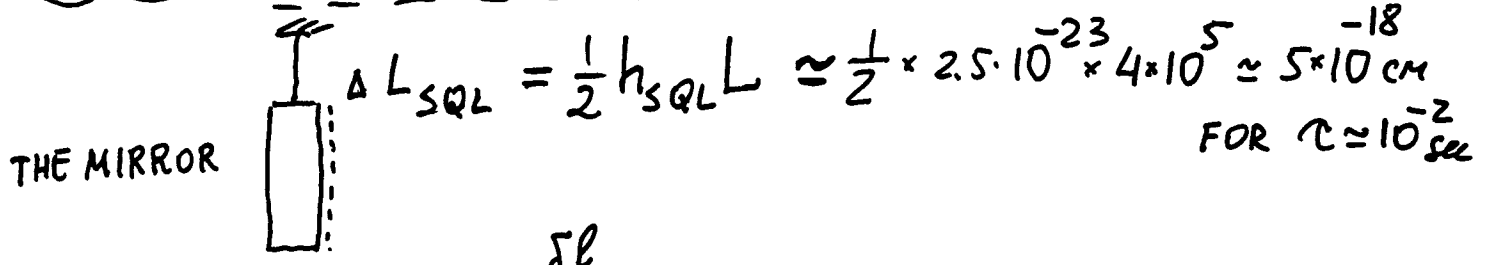


Figure 5.
Typical shape of the excess noise event.

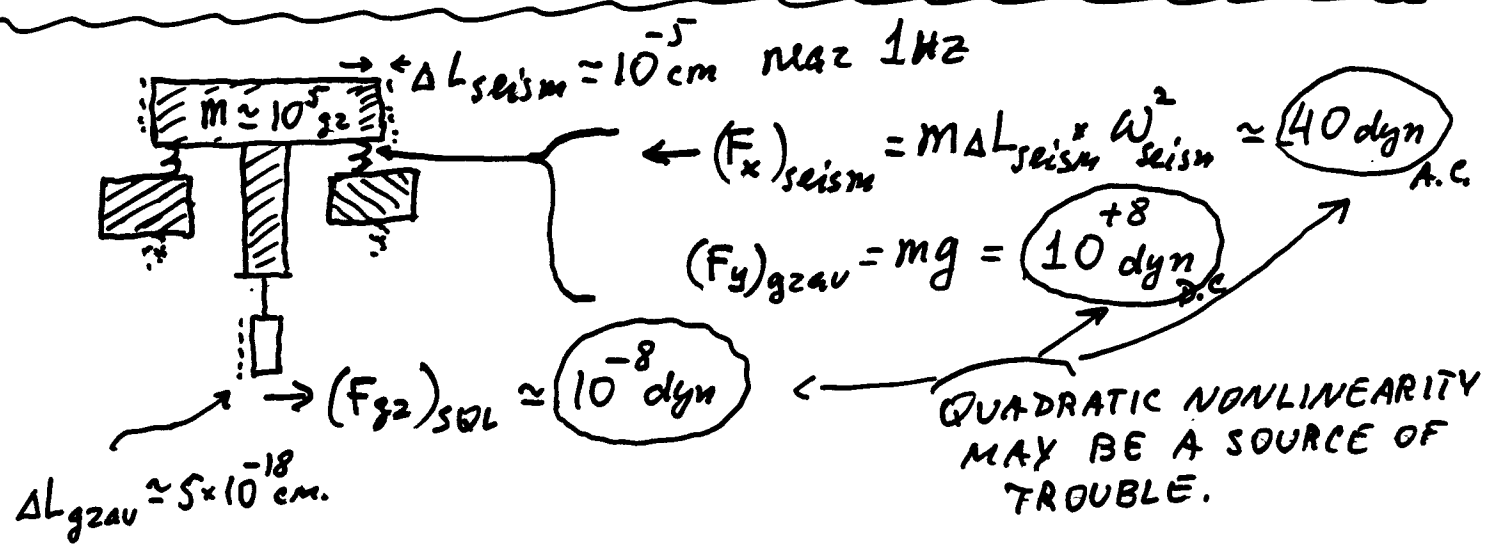
In 1997 the steel wires noise will be tested.
 In 1997/1998 the fused silica fiber's noise
 will be tested.

2. 3.

Several numerical considerations



$\Delta L_{SQL} \approx 5 \cdot 10^{-18} \text{ cm}$
 $\tau \approx 10^{-2} \text{ sec}$ } compare WITH $\delta l \approx 2 \cdot 10^{-10} \text{ cm}$
 $\tau \approx 10^{+3} \text{ sec}$



It is likely that the output will demonstrate a polymodal, and nonstationary signal noise

Thus it will be a problem to establish the level of confidence when the signal is recorded.